Smart Structures and Systems, *Vol. 29, No. 3 (2022) 433-444*
https://doi.org/10.12989/sss.2022.29.3.433

Prediction of long-term compressive strength of concrete with admixtures using hybrid swarm-based algorithms

Lihua Huang*[1], Wei Jiang [2], Yuling Wang [1], Yirong Zhu [3] and Mansour Afzal [4]

[1] *School of Management Engineering, Zhejiang Guangsha Vocational and Technical University of Construction, Dong Yang, 322100, China*
[2] *School of Intelligent Manufacturing, Zhejiang Guangsha Vocational and Technical University of Construction, Dong Yang, 322100, China*
[3] *Glodon Company Limited, Beijing, 100193, China*
[4] *Islamic Azad University, Ardabil, Iran*

(*Received November 19, 2020, Revised September 29, 2021, Accepted November 24, 2021*)

Abstract. Concrete is a most utilized material in the construction industry that have main components. The strength of concrete can be improved by adding some admixtures. Evaluating the impact of fly ash (FA) and silica fume (SF) on the long-term compressive strength (CS) of concrete provokes to find the significant parameters in predicting the CS, which could be useful in the practical works and would be extensible in the future analysis. In this study, to evaluate the effective parameters in predicting the CS of concrete containing admixtures in the long-term and present a fitted equation, the multivariate adaptive regression splines (MARS) method has been used, which could find a relationship between independent and dependent variables. Next, for optimizing the output equation, biogeography-based optimization (BBO), particle swarm optimization (PSO), and hybrid PSOBBO methods have been utilized to find the most optimal conclusions. It could be concluded that for CS predictions in the long-term, all proposed models have the coefficient of determination (R^2) larger than 0.9243. Furthermore, MARS-PSOBBO could be offered as the best model to predict CS between three hybrid algorithms accurately.

Keywords: fly ash; high strength concrete; long-term CS prediction; MARS-BBO; MARS-PSO; MARS-PSOBBO; silica fume

1. Introduction

One of the most popular materials used in construction fields such as buildings, pavements, and infrastructures is concrete. The main constituents of standard concrete are coarse aggregate (CA), fine aggregates, ordinary portland cement (OPC), and water. Recently, alternative materials such as silica fume (SF), fly ash (FA), nano-zeolite, etc., were used to surge the sustainability of concretes, regarding the reduction of the carbon dioxide emission percentage corporate with the utilization of by-products materials (Esmaeili-Falak *et al*. 2020a). It has been proven that cement plants contribute to roughly 5–7% of the universal CO_2 emission (Benhelal *et al*. 2013). Moreover, although standard concrete is widely used in the construction industry, in some special situations like skyscrapers, pavements, and long-span bridges, concretes may include some disadvantages around strength, workability, and durability.

Research on using mineral admixtures, especially FA and SF, to improve concrete mechanical properties has been under consideration for many years (Toutanji *et al*. 2004). Because many mineral admixtures are by-products from other industries, these waste materials would be better to be used to decrease the amount of cement, which causes reducing the cost of concrete production and includes environmental advantages. FA was replaced with cement in the concrete from 20% (low volume) to 50% (high volume) (Lam *et al*. 1998). Moreover, it has been reported that FA has adverse effects on the CS, especially at early age of concrete. Furthermore, FA could be replaced by up to 60% if early age strength is not a significant factor (Babu and Rao 1994). When concrete is prepared under low water conditions, it may result in high strength performance. Siddique (2004) has reported that although the concrete made of FA resulted in a lower modulus of elasticity to control concrete at 7 and 14 days, it showed a virtually higher modulus of elasticity at 90 days.

Moreover, it has been shown that using FA reduces the initial strength in the short term, and generally, this reducing trend decreased with the amount of FA replacement increments (Siddique 2004). It is worth considering that using FA at high percentages causes a high adhesion paste, where reduces workability of concrete, and needs superplasticizer. Therefore, the proportion of mixed design of concretes with admixtures must be optimized in either durability or workability (Cabrera and Claisse 1990).

SF, because of its small particle size, plays a dual role as a filler and pozzolan in the concrete (Turk *et al*. 2010). It has been shown that increasing volume ratio of SF in the concrete mixture leads to improve mechanical properties at different ages (Felekoğlu *et al*. 2007, Hubertova and Hela 2007). Generally, it is accepted that some range of SF can significantly raise CS, reduce permeability, and prevent

*Corresponding author, Ph.D.,
E-mail: huanglihua6176@163.com

ISSN: 1738-1584 (Print), 1738-1991 (Online)

corrosion in reinforced structures. Some researchers have reported that the significant impact of SF on mechanical properties occurs between 3 and 28 days. In spite, an optimum SF value in the mix has not been reported in the same proportion so far (Detwiler *et al*. 1996, Kjellsen *et al*. 1999). Self-consolidating concrete has been studied by Mohamed and Najm (2016), in which a large proportion of cement (80%) was replaced with various combinations of FA, SF, and slag. They resulted that the mix consisting of 15% FA-15% SF -50% slag has the best CS for 3 to 28 days.

Since the last two decades, various predicting approaches based on artificial intelligence (AI) have been widely used and developed by many researchers for a wide range of engineering applications (Esmaeili-Falak *et al*. 2019, Oreta and Ongpeng 2011). For developing an AI model, the more series of experimental test results with different proportions, the higher efficiency, acceptance, more robust, and lower errors. In other words, the developed model would be able to predict experiments' results in the future using the previous results with a high rate of accuracy if test results were exact. Moreover, the concluded model would be capable (Chou and Ghaboussi 2001). Modeling the classical approaches have analyzed the impact of SF on the CS. Unfortunately, these models have not been progressed to forecast the CS of concrete precisely (Nochaiya *et al*. 2010). Additionally, it is not possible to assess the exact effect of each parameter on the CS by using the methods mentioned above unless some new approaches have been considered. The result of artificial network models and optimizing algorithms has presented an appropriate estimation of CS of concrete in the long-term containing FA and SF, which could help expand and determine the achievement of concrete engineering goals (Pala *et al*. 2007, Topcu and Sarıdemir 2008, Yaprak *et al*. 2013, Atici 2011, Chou and Pham 2013).

Regarding the CS of high-performance concrete (HPC), Yeh (1998) proposed the probability of using an artificial neural network (ANN) for the prediction of CS containing FA and blast furnace slag. Several researchers also utilized ANN for forecasting the CS containing FA (Benemaran and Esmaeili-Falak 2020). Gene Expression Programming algorithm was applied by Mousavi *et al*. (2012) to predict the CS with FA. In another study, because the hierarchical structures have better structure compared to flat ones, a combination of regression and classification techniques such as support vector machine (SVM) and ANN was used to increase the efficiency of CS prediction models (Azimi-Pour *et al*. 2020). In 2017, the successful operation of the M5P model tree method for forecasting the CS of the HPC had been reported by Behnood *et al*. (2017).

In general, HPC's porosity and CS are lower and higher than NC's, respectively. The value of CS could be gathered from experimental tests or predictive models, which is needed in many design codes. Predictive models can help produce sufficient data, which causes saving energy, cost, and time (Esmaeili-Falak 2017, Sarkhani Benemaran *et al*. 2020, Sarkhani Benemaran 2017). In recent decades, more researchers have proposed equations and predicted models about the prediction of the CS of normal and high-performance concrete. Due to the differences in mixture constituents and hardened proportions, the acceptance rate of these models to predict the CS of HPC is challenging. Hence, developed models to predict CS of the HPC would be needed to result in reliable forecast values. Moreover, a comprehensive dataset that includes mixture constituents is necessary to develop dependable models.

The two used methods to forecast the CS of concrete were the traditional statistical method and the non-linear prediction method (Zelić *et al*. 2004). Nowadays, because a different type of admixtures has been applied widely in concrete, which is used as inputs, the relationship between the input factors and the output mechanical properties (CS and TS) is more complex and non-linear (Wang *et al*. 2014, Esmaeili-Falak *et al*. 2017, 2020b). Consequently, previous methods are not highly appropriate for forecasting the CS of concrete. In such studies, a restricted number of components have been considered by authors. Other appropriate methods should be taken to propose a relationship between mixed components and mechanical properties. However, machine learning methods such as MARS or regression solutions using deep learning have been developed for forecasting mechanical properties. They hence would be an efficient approach for multi-admixture concrete (Khademi *et al*. 2017). In other words, applying understandable mathematical formulas by considering effective parameters in estimating CS, which could be obtained from MARS and optimized using optimization methods such as Biogeography-based optimization (BBO), particle swarm optimization (PSO), or hybrid algorithms could have better application in practical works in order to design optimized mixture (Moayedi *et al*. 2019, Shariati *et al*. 2019).

In this study, the datasets were provided to evaluate the effect of FA and SF on the CS of concrete in the long-term. The MARS method has been used to evaluate the effective parameters in predicting the CS of concrete containing FA and SF and present a fitted equation. For this purpose, binder content (B), fly ash to binder ratio (FA/B), silica fume to binder ratio (SF/B), coarse aggregate to binder ratio (CA/B), coarse aggregate to the total aggregate ratio (CA/TA), water to binder ratio (W/B), superplasticizer to binder ratio (SP/B) and curing time (CT) (days) are as input variables and the CS is defined as output variable. Next, for optimizing the output equation, MARS-BBO, MARS-PSO, and MARS-PSOBBO optimization methods have been used to modify the coefficients of the extracted equation to provide an optimal model with the appropriate error results. In order to evaluate the accuracy of the used method to estimate the CS of the concrete and the effect of optimizer algorithms, four statistical criteria were used.

2. Datasets and methodologies

2.1 Description of the datasets

In order to assess the influence of FA and SF on the CS of concrete in long-term (28, 56, 90, and 180 days), an experimental-based dataset including 96 data records was

Table 1 The statistical values of the input and output variables

Features	Descriptive indexes						
	Minimum	Maximum	Mean	St. deviation	Median	Variance	Skewness
B (kg)	400	500	436/67	45/21	410	2022/2	0/69193
FA/B	0	0/55	0/25	0/191	0/225	0/03625	0/1104
SF/B	0	0/05	0/0187	0/0243	0	0/000586	0/5246
CA/B	2/172	2/9	2/61	0/315	2/761	0/09814	-0/06246
CA/TA	0/6	0/68	0.638	0/022	0/6364	0/000505	0/06966
W/B	0/3	0/5	0/4	0/082	0/4	0/006667	1/13e-15
SP/B (%)	0	2/6	1/06	0/83	1/3375	0/6767	-0/1315
CT	28	180	88/5	57/51	73	3272	0/6922
$f_{cs\text{-}28}$ (MPa)	24	87/8	58/24583	18/11137	56/65	314/35	0/1914
$f_{cs\text{-}56}$ (MPa)	33/7	94/8	65/9125	16/096829	62/1	275/93	0/215
$f_{cs\text{-}90}$ (MPa)	41/4	99/6	70/6	16/39	67/9	257/5	0/29
$f_{cs\text{-}180}$ (MPa)	48/3	107/8	75/53	17/10	70/4	280/24	0/5814

selected from a published study (Lam *et al*. 1998). Different parameters that can influence the value of the CS were considered as input variables, including, B: binder content (kg), FA/B: fly ash to binder ratio, SF/B**:** silica fume to binder ratio, CA/B: coarse aggregate to binder ratio, CA/TA: coarse aggregate to total aggregate ratio, W/B: water to binder ratio, SP/B: superplasticizer to binder ratio (%), and CT: curing time. In Table 1, the statistics of the input and output variables are presented.

2.2 Multivariable Adaptive Regression Splines (MARS)

The MARS method is one of the unique approaches to use for prediction purposes. MARS is a nonparametric modeling technique that works without any assumptions about the relationship between independent (inputs) and dependent (outputs) variables (Dutta *et al*. 2018). Through the model procedure, the MARS technique segments the training datasets into several splines with an identical interval basis. Then, it makes a linear regression equation for each region (Friedman 1991). The breaks between regions are called "knots," and the term "basis function (BF)" presents each distinct interval of the predictors. The general form of the BF is: "max (0, k-X) or max (0, X-k)", where "X" is input, and "k" is a constant from regression lines. In this study, the MARS algorithm has provided using independent variables (inputs) (X) = [B, FA/B, SF/B, CA/B, CA/TA, W/B, SP/B, CT] to produce a series of BFs and then applied them to the output (compressive strength). A MARS model is developed in two base steps as follows:

1. Firstly, the MARS algorithm calculates the general formulation of the MARS with Eq. (1).
2. Secondly, because of the probability of overtraining during the above step, the backward algorithms check the proposed model by removing extra basis BFs. The extra BFs are deleted by Generalized Cross-Validation (GCV), according to Eq. (2) (Craven and Wahba 1978).

$$E = c_0 + \sum_{n=1}^{N} c_m BF_m(x) \tag{1}$$

$$GCV\ (N) = \left(\frac{1}{n} \frac{\sum_{m=1}^{N} (y_i - \hat{y}_i)^2}{\left(1 - \frac{C(M)}{n}\right)^2} \right) \tag{2}$$

$$C(M) = M + dM \tag{3}$$

x	independent variable
c_0	constant
c_m	coefficient of BF(x) (Adamowski 2008)
n	number of the data object
y_i	response value of object (i)
$\hat{y}_i$	predicted response value of object (i)
C (M)	penalty factor
d	the cost penalty factor of each basis function optimization
M	maximum number of BFs in the model

The limitation of this methods is that the resulted equation is highly dependent of dataset. However, it has been tried to cover wide range of variables to increase the generality of results.

2.3 Particle Swarm Optimization (PSO)

PSO algorithm introduced by Kennedy and Eberhart (1995) is an evolutionary computation technique that uses a non-linear procedure to solve the problem. The basic concept of PSO derivates from a simulation of the social behavior of a flock of birds or fish swarms. In PSO, solutions were depicted as particles flying in the problem search area to find their best position. Each particle's positions were updated based on the best positions of particles in each iteration. Hence, PSO must also include a fitness evaluation function that can get the position of

particles and ascertain a fitness value to it. After the K[th] iteration, the swarm was updated using Eqs. (4)-(5).

$$V_i^{k+1} = \rho^k V_i^k + c_1 r_1 \left(P_i^k - X_i^k\right) + c_2 r_2 (P_g^k - X_i^k) \quad (4)$$

$$X_i^{k+1} = X_i^k + V_i^{k+1} \quad (5)$$

X_i current position
V_i velocity vectors of the i[th] particle
P_i best previous position of the i[th] particle
P_g best global position among all of the particles
$r_1,\ r_2$ uniform random sequences generated from the interval [0,1]
$c_1,\ c_2$ cognitive and social scaling parameters
ρ^k inertia weight

The inertia weight ρ^k may be determined to alter linearly from a maximum value ρ^{max} to minimum value ρ^{min}. Velocity vector V_i is limited to a lower bound V^l and upper bound V^u. The whole process of the MARS-PSO method of optimization is clarified in Fig. 1. According to the provided flowchart, reaching the final iterative step is the optimization terminated point. The try and error method is applied to adjust the maximum iteration and population numbers for achieving a strong convergence of the cost function.

2.4 Biogeography-based optimization (BBO)

The BBO method is one of the meta-heuristic optimization algorithms developed by Simon (2008). BBO algorithm is inspired by the geographical distribution, emigration, and immigration of species in an ecosystem. In this method, it is assumed that an ecosystem includes a restricted number of habitats. Many factors-called suitability index variables (SIVs)-affect the quality of habitat for species, including food, water resources, climatecondition, etc. (Esmaeili-Falak *et al*. 2018, Poorjafar *et al*. 2021). The quality of each habitat is represented by the habitat suitability index (HSI). When a habitat is saturated or has a large HIS, the species are inclined to emigrate from this habitat and immigrate to the low value of HIS. Each habitat depicted one possible answer for the problem, and its suitability indexes are the decision variables (DVs). In the minimization procedure, the solutions with lower objective values have higher values of HSIs. Two operators, “migration” and “mutation”, are used in this algorithm. The migration operator is used to explore the neighborhood of the available solutions; however, the mutation operator is utilized to find the new solutions and to assist the exploration.

For habitats with the size of HS, the habitats are sorted from their cost function values. The suitability of the i[th] habitat (HSI_i) in the sorted population is defined as Eq. (6).

$$HSI_i = -i + HS + 1 \quad (6)$$

The emigration (μ_i) and immigration (λ_i) values are computed using Eqs. (7)-(8).

$$\mu_i = \frac{HSI_i}{HS} \quad (7)$$

$$\lambda_i = 1 - \frac{HSI_i}{HS} \quad (8)$$

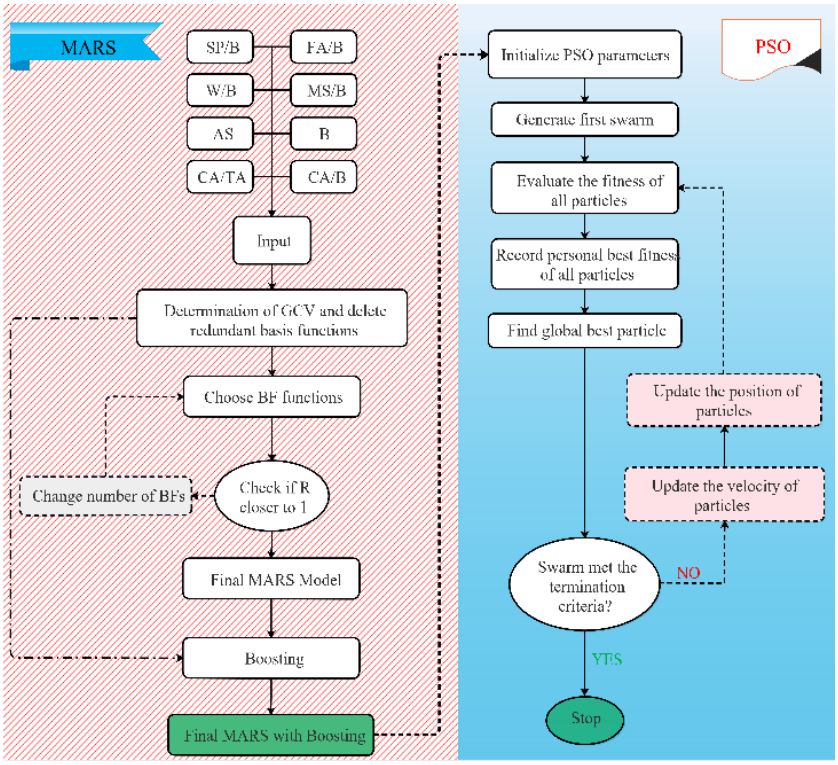

Fig. 1 Flowchart of MARS-PSO

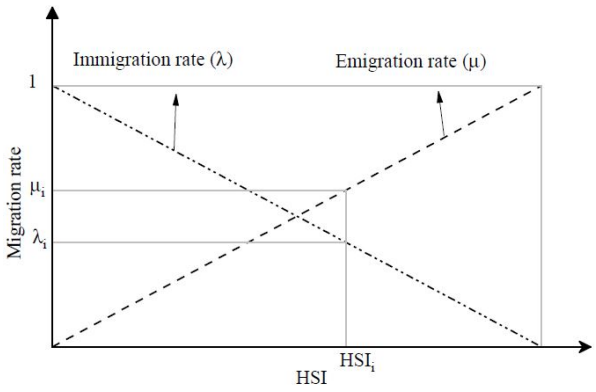

Fig. 2 Migration curve of the BBO algorithm

In Fig. 2, the migration curve of the BBO method is presented. In this study, the maximum values of the emigration and immigration rates are assumed to be one. The whole process of the MARS-BBO method is clarified in Fig. 3.

Migration from the j^{th} decision variable of r^{th} habitat to the decision variable of i^{th} habitat is formulated using Eq. (9).

$$DV_j^k = \alpha DV_j^i + (1-\alpha)DV_j^r \quad (9)$$

2.5 A hybrid optimization algorithm: PSOBBO

The combination of BBO with PSO as a novel hybrid technique was primarily merged through biogeography-based particle swarm optimization (BPSO) proposed by Guo *et al*. (2014). The PSO has a powerful capability of exploration. However, BPSO does mainly neglect its dominance since BBO performs the optimization, and PSO exploration is not accomplished for all iterations. Therefore, in this section, a novel hybrid optimization algorithm based on BBO and PSO combination applying an efficient and different hybridization strategy is proposing. Moreover, the benchmark function tests are utilized to assess the optimization performance of the proposed algorithm.

The whole initial population will be applied to both PSO and BBO. The PSO will be first employed to implement global exploration independently. In this way, the whole population will converge to a decent local optimum. Then BBO will be employed for local search by setting the global best positions and global best costs of the individuals in BBO as the local optima achieved by PSO. The number of individuals in BBO is equal to the number of local optimums. The PSO individuals will converge at the global best position, which will be recorded as an optimization result.

Exploration and exploitation are two critical criteria in the optimization process. In PSOBBO, PSO is utilized to explore the whole solution space while BBO is employed to exploit the local optima. In this way, the novel proposed hybrid optimization makes a reasonable balance between exploitation and exploration. It creates a robust search capacity in the solution space and provides superior performance of the optimization procedure. The framework of PSOBBO is illustrated in Fig. 4.

2.6 Performance evaluation methods

In order to evaluate the accuracy of the used method to estimate the CS and TS of the concrete and the effect of

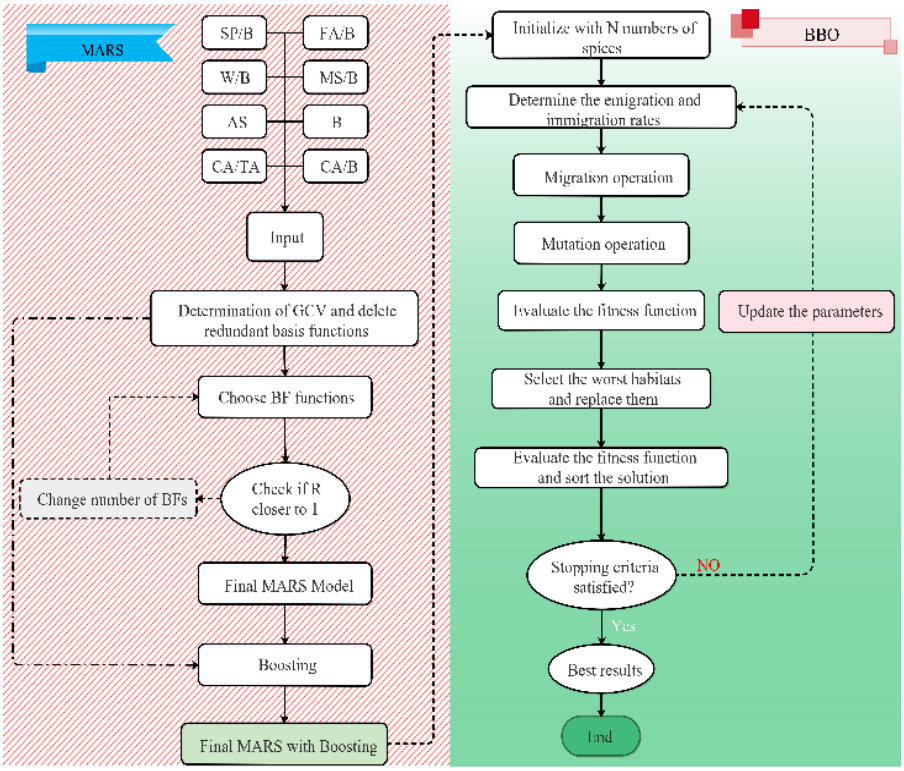

Fig. 3 Flowchart of MARS-BBO

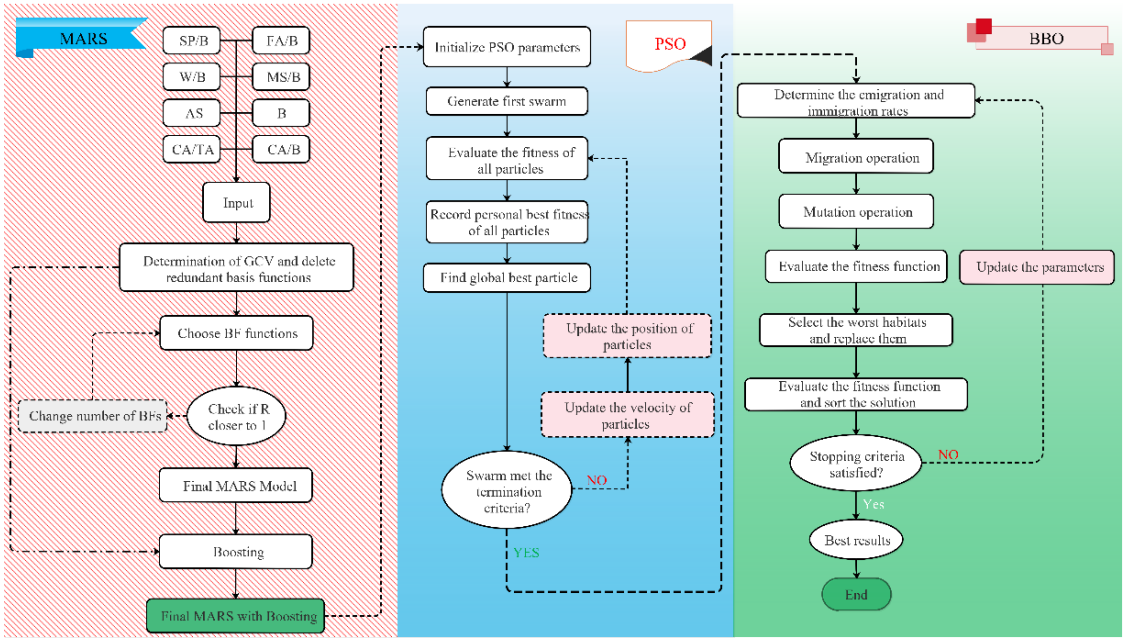

Fig. 4 Flowchart of MARS-PSOBBO

optimizer algorithms, four statistical criteria including the Root Mean Squared Error (RMSE), the Mean Absolute Error (MAE), the coefficient of determination (R^2), the Mean Absolute Percentage Error (MAPE), and performance index (PI) were used, which are defined as follows in Eqs. (10)-(14).

$$RMSE = \sqrt{\frac{1}{P}\sum_{p=1}^{P}(y_p - t_p)^2} \tag{10}$$

$$MAE = \frac{1}{P}\sum_{p=1}^{P}|y_p - t_p| \tag{11}$$

$$R^2 = \left(\frac{\sum_{p=1}^{P}(t_P - \bar{t})(y_P - \bar{y})}{\sqrt{\left[\sum_{p=1}^{P}(t_P - \bar{t})^2\right]\left[\sum_{p=1}^{P}(y_P - \bar{y})^2\right]}}\right)^2 \tag{12}$$

$$MAPE = \frac{1}{P}\sum_{p=1}^{P}\left|\frac{y_P - t_P}{y_P}\right| \tag{13}$$

$$PI = \frac{1}{|\bar{t}|}\frac{RMSE}{\sqrt{R^2 + 1}} \tag{14}$$

y_P the predicted values of the P^{th} pattern
t_P the target values of the P^{th} pattern
$\bar{t}$ the averages of the target values
$\bar{y}$ the averages of the predicted values

3. Results and discussion

In civil projects, because of the high-volume consumption of the concrete and the nature of practical works, a mathematical equation is much more useful than having a computer model. Moreover, a mathematical model could be used by researchers, and its parameters and coefficients simply could be assessed and modified. Meanwhile, at the moment, the machine learning methods could obtain more real consequences than other empirical methods for model development. In contrast, the main disadvantages of these methods are the black-box nature of them, which does not allow us to have a conception about how the problem is solved, and just the final results are accessible. However, there are other machine learning algorithms that either solve the problem with high efficiency or give us an equation. These algorithms are known as white-box methods, where researchers could access an equation as a solution. One of the white-box algorithms is the MARS algorithm; therefore, the developed model enables the researchers to find the critical parameters in their analysis and use the correct model in future studies.

In this study, the datasets were provided to develop a new model based on mathematical terms, which are not only usable in practical works, but also are extensible in future analysis. Evaluating the significant parameters to predict the CS of concrete in long-term containing mineral admixtures and to present a fitted equation, the MARS method has been used. In the next step, optimizing the output equation, optimization methods such as BBO, PSO, and hybrid PSOBBO have been used to modify the extracted equation's coefficients to provide an optimal model with the appropriate error upshots.

To train new MARS models for estimation CS in the long-term and to assess them, 80% of datasets were used to train, and 20% of the rest was used for the model validation. Furthermore, using this method, the base parameters affect

to predict the CS could be obtained from their coefficients and the number of inputs' repetition in the equation. Input variables are B, FA/B, SF/B, CA/B, CA/TA, W/B, SP/B, CT (28, 56, 90, and 180 days), and experimental CS to develop MARS model for exploring accurate equation and useful parameters; several trial and error processes were considered to obtain the best MARS model setting for this problem. The final model for predicting CS was obtained as Eq. (15). By analyzing the output model, it resulted that the parameters of CA/TA, CT, CA/B, FA/B, B, and SP/B (%) had the strongest impression on the estimation of CS (f_{CS}).

MARS:

$$\begin{aligned} f_{CS} = & -652.550 + 1110.1971 \times \max\left(0, \frac{\mathrm{CA}}{\mathrm{TA}} - 0.6\right) \\ & + 0.10313 \times \max(0, \mathrm{CT} - 28) \\ & + 975.8197 \times \max\left(0, \frac{\mathrm{CA}}{\mathrm{B}} - 2.172\right) \\ & - 87.843 \times \max\left(0, \frac{\mathrm{FA}}{\mathrm{B}}\right) \\ & + 7.578616 \times \max(0, \mathrm{B} - 400) \\ & - 9.6976 \times \max\left(0, \frac{\mathrm{SP}}{\mathrm{B}}\right) \end{aligned} \quad (15)$$

Also, three optimization algorithms were used to increase the accuracy of the prediction equation adopted from MARS. For this purpose, optimizing the output equation, optimization methods such as BBO, PSO, and hybrid PSOBBO have been used as integrated algorithms to modify the extracted equation's coefficients to provide an optimal model appropriate result. Moreover, some previous studies have developed AI methods for CS prediction, which consequence in the development of black boxes without a practical potential to be used in future applications, hence only "prediction" was implied instead of model development tries. The Eq. (15) were optimized using the mentioned integrated algorithms and reported in Eqs. (16)-(18) for CS that are related to MARS-PSO, MARS-BBO, and MARS-PSOBBO, respectively.

MARS − PSO:

$$\begin{aligned} f_{CS} = & -662.937 + 1109.735 \times \max\left(0, \frac{\mathrm{CA}}{\mathrm{TA}} - 0.020\right) \\ & + 0.103 \times \max(0, \mathrm{CT} - 28) \\ & + 957.441 \times \max\left(0, \frac{\mathrm{CA}}{\mathrm{B}} - 2.830\right) \\ & + 103.152 \times \max\left(0, \frac{\mathrm{FA}}{\mathrm{B}} - 0.077\right) \\ & + 1.134 \times \max(0, \mathrm{B} - 396.614) \\ & - 7.425 \times \max\left(0, \frac{\mathrm{SP}}{\mathrm{B}} - 0.124\right) \end{aligned} \quad (16)$$

MARS − BBO:

$$\begin{aligned} f_{CS} = & -667.017 + 1068.38 \times \max\left(0, \frac{\mathrm{CA}}{\mathrm{TA}}\right) \\ & + 0.10242 \times \max(0, \mathrm{CT} - 28) \\ & + 975.218 \times \max\left(0, \frac{\mathrm{CA}}{\mathrm{B}} - 2.8312\right) \\ & - 98.9673 \times \max\left(0, \frac{\mathrm{FA}}{\mathrm{B}} - 0.075\right) \\ & + 1.1344 \times \max(0, \mathrm{B} - 391.426) \\ & - 9.2037 \times \max\left(0, \frac{\mathrm{SP}}{\mathrm{B}} - 0.2389\right) \end{aligned} \quad (17)$$

MARS − PSOBBO:

$$\begin{aligned} f_{CS} = & -665.893 + 1101.84 \times \max\left(0, \frac{\mathrm{CA}}{\mathrm{TA}}\right) \\ & + 0.10283 \times \max(0, \mathrm{CT} - 28) \\ & + 962.83 \times \max(0, \mathrm{CA/B} - 2.851)) \\ & - 104.183 \times \max\left(0, \frac{\mathrm{FA}}{\mathrm{B}} - 0.07325\right) \\ & + 1.052 \times \max(0, \mathrm{B} - 414.555) \\ & - 18.7121 \times \max\left(0, \frac{\mathrm{SP}}{\mathrm{B}} - 2.0997\right) \end{aligned} \quad (18)$$

One of the best ways to evaluate the accuracy and efficiency of designed models is comparing performance evaluation results by considering RMSE, MAE, R^2, and MAPE between the first model and integrated algorithms. Based on the performance evaluation results from Table 2, it can be seen that R^2, RMSE, MAE, and MAPE value for simple MARS model to predict CS in long-term is 0.9243, 4.9406, 3.9099, and 4.8678e-5, respectively, which indicates that the proposed MARS model has a prediction ability with reasonable accuracy. By implying optimization algorithms to simple MARS, from Table 3, it is observed that R^2, RMSE, MAE, and MAPE for MARS-PSOBBO has the best values at 0.9422, 4.3169, 3.5, and 6.2176e-5 than simple MARS, which R^2 and MAPE are 1.9 and 27.73% larger and RMSE and MAE are 12.63 and 10.48 % lower respect to simple MARS. Furthermore, MARS-PSO has the second highest performance with 1.63 and a 36% rise for R^2, and 10.47 and 8.62% decline for RMSE and MAE. Furthermore, the performance evaluation results of MARS-BBO had acceptable responses with a low difference with MARS-PSO. This shows that for this kind of problem, the proposed algorithms would be useful enough, and, remarkably, hybrid MARS-PSOBBO showed its effectiveness in optimization applications, and its resulted equations are more reliable.

Generally, all approaches provided virtually acceptable performance when predicting CS in the long-term. However, MARS-PSOBBO was better than MARS-PSO and MARS-

Table 2 Performance measurements for CS of concrete

Method	R2	Rank for R^2	RMSE	Rank for RMSE	MAE	Rank for MAE	MAPE	Rank for MAPE	PI	Rank for PI
MARS	0.9243	4	4.9406	4	3.9099	4	0.0049	2	0.0373	4
MARS-BBO	0.9389	3	4.4387	3	3.5829	3	0.0016	3	0.0334	3
MARS-PSO	0.9394	2	4.4229	2	3.5729	2	7.899e-6	4	0.0332	2
MARS-PSOBBO	**0.9422**	1	**4.3169**	1	**3.5**	1	**0.0062**	1	**0.0324**	1

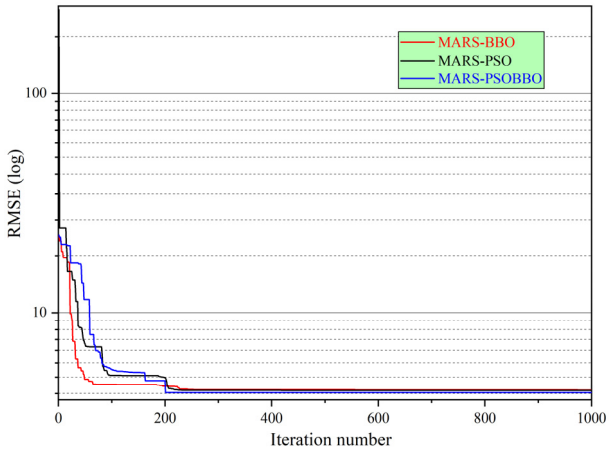

Fig. 5 Convergence curves for proposed prediction models of CS

BBO in terms of learning convergence speed and final result. To make sense, the relationship between RMSE and the number of iterations for three proposed methods are illustrated in Fig. 5 for CS. According to Fig. 5, in modeling CS the convergence of MARS-PSOBBO is faster than MARS-BBO, and this is faster than MARS-PSO and the final value with the lowest cost function belongs to MARS-PSOBBO. However, although the convergence speed of MARS-BBO is higher than MARS-PSO, the final RMSE value for MARS-PSO is approximately better than MARS-BBO that this difference is negligible, which MARS-BBO could be proposed better method than MARS-PSO in this kind of problem. For example, at the value of RMSE4.723 MPa, MARS-BBO needs to run around 70 iterations, while MARS-PSO needs just above 200 iterations.

Moreover, not only MARS-PSOBBO convergence speed was very high, but also its RMSE value was the lowest one. On the other hand, at the same iteration after convergence, MARS-PSOBBO shows better performance than MARS-PSO and MARS-BBO. For example, after iteration 400, MARS-PSOBBO is stable at a value of RMSE 4.3169, while MARS-PSO and BBO converge at RMSE 4.4229 and 4.4387, respectively, which show 2.45% and 2.82% higher in RMSE.

Experimental and predicted results developed by MARS, MARS-BBO, MARS-PSO, and MARS-PSOBBO for 28-, 56-, 90- and 180-days f_{CS} results were given in Fig. 6. As shown in Fig. 6, the values for long-term CS obtained before and after optimization are very close to the experimental results. By comparing results, fitted equation and optimization methods have a remarkably appropriate influence on increasing coefficient of determination. This case proves that the experimental results with proposed and optimized equations are all in harmony, in which the PSOBBO algorithm has the highest positive effect.

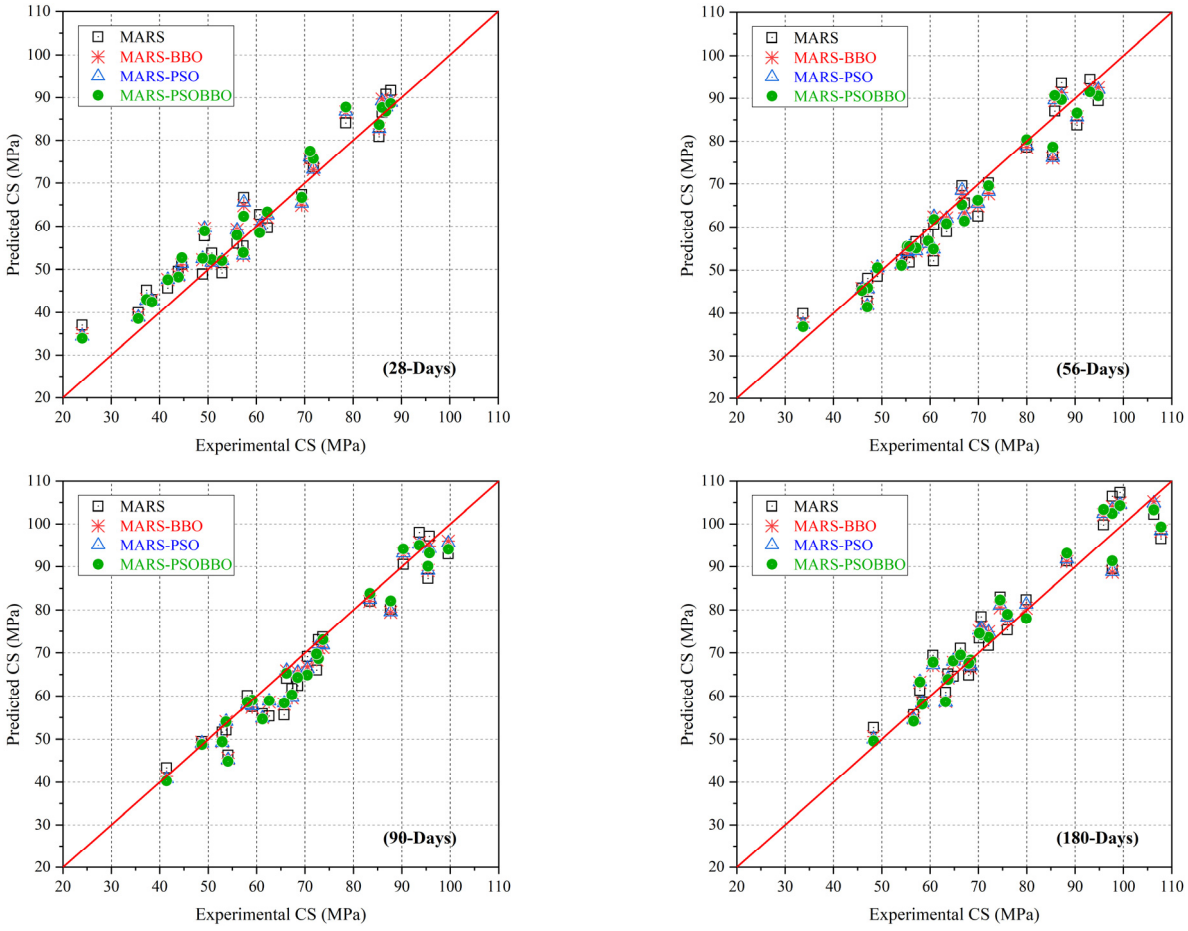

Fig. 6 Predicted 28-, 56-, 90, and 180 days CS of different models vs. experimental results

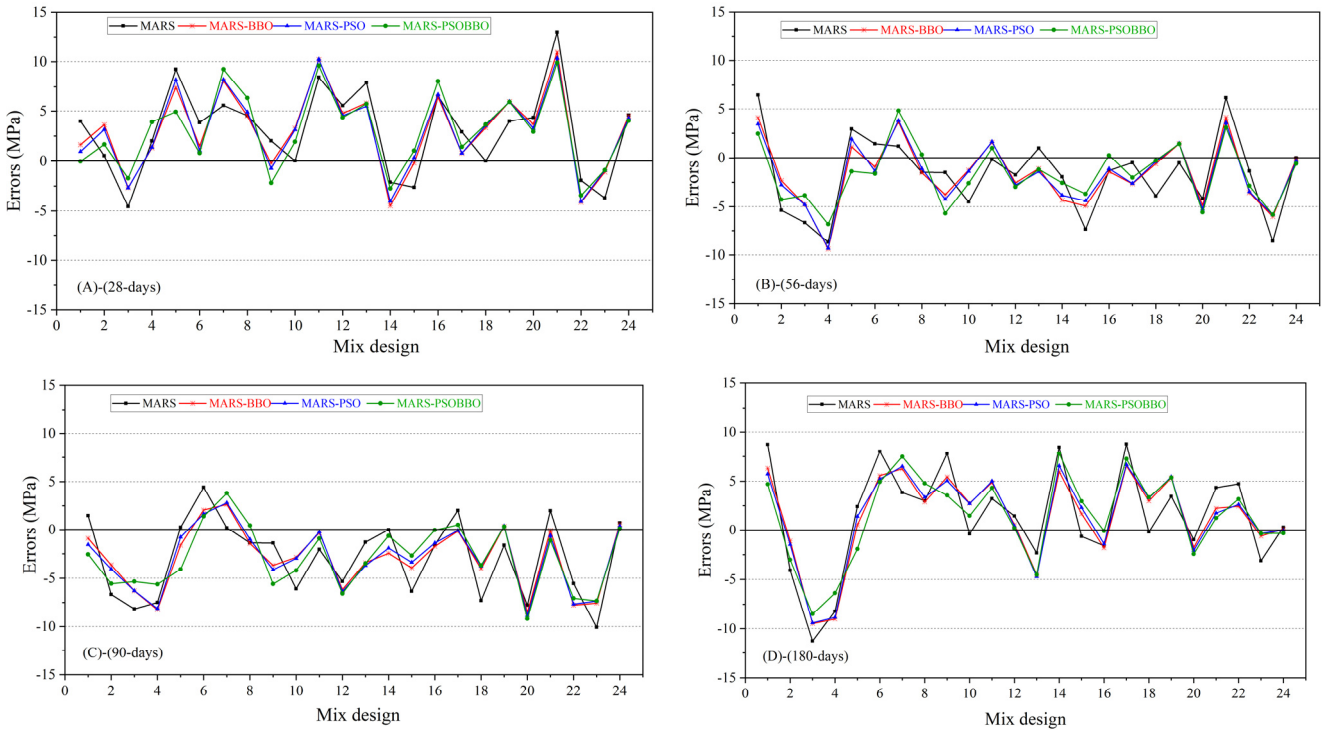

Fig. 7 Errors in the different methods for various CT: (a) 28-days; (b) 56-days; (c) 90-days; and (d) 180-days

Furthermore, Figs. 7(a)-(d) compare the differences between experimental results of CS with simple MARS and optimized results for different CT. As it is observed from Figs. 7(a)-(d), for all CT, MARS-PSOBBO has the greatest number of mix designs that have lower errors compared to other algorithms, which represents the efficiency of this hybrid method. It is also evident that the maximum error within samples is 12.9 MPa for simple MARS. The other mix designs are in the limitation of 10 MPa, where it was reduced as possible by optimization algorithms, especially PSOBBO at a higher decline percentage. The given Fig. 8 depicts the error histogram in cumulative form for developed models. Regarding error histograms, the more instances around error zero line, the highest capability of model. The given error distribution figures represent that error distribution curves are like the Gaussian bell.

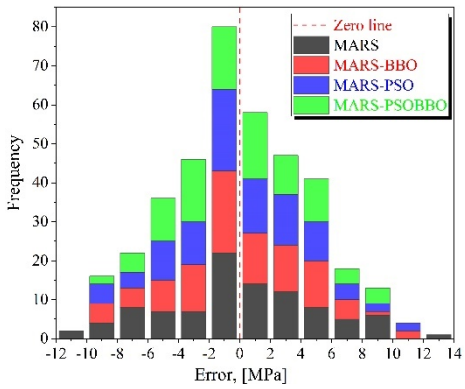

Fig. 8 Error histogram in cumulative form for developed models

The experimental CS and the predicted values from the simple (MARS) and optimized models (MARS-BBO, MARS-PSO, MARS-PSOBBO) are provided in Figs. 9(a)-(d), respectively. At these figures, mixed design number from 1 to 24 belong to 28-day age of samples, 25-48 are results of 56-day age, 49-72 are for 90-day samples, and 73-96 are results of 180-day age. The given figures illustrate that the values determined from models are well correlated to the experimental CS values. However, the hybrid PSOBBO algorithm results have the highest correlation between measured and predicted CS, which could be presented as the proposed model.

4. Conclusions

In this study, the datasets were provided to develop a new model based on mathematical terms to evaluate FA and SF's effect on the CS of concrete in the long-term, which are usable in practical works, and are extensible in the future analysis. The MARS method has been used to evaluate the effective parameters in the forecast of the CS of concrete containing FA and SF in the long-term and to present a fitted equation. For this purpose, B, FA/B, SF/B, CA/B, CA/TA, W/B, SP/B, and CT are input variables, and the CS are defined as output variables. Next, by optimizing the output equation, MARS-BBO, MARS-PSO, and hybrid MARS-PSOBBO optimization methods have been used to modify the extracted equation's coefficients and provide an optimal model with the appropriate error results. It could be concluded that for predictions CS, all models could predict results with high accuracy, with R^2 equals to 0.9243. However, between three hybrid algorithms, MARS-PSOBBO (Eq. (19)) could be proposed as the best

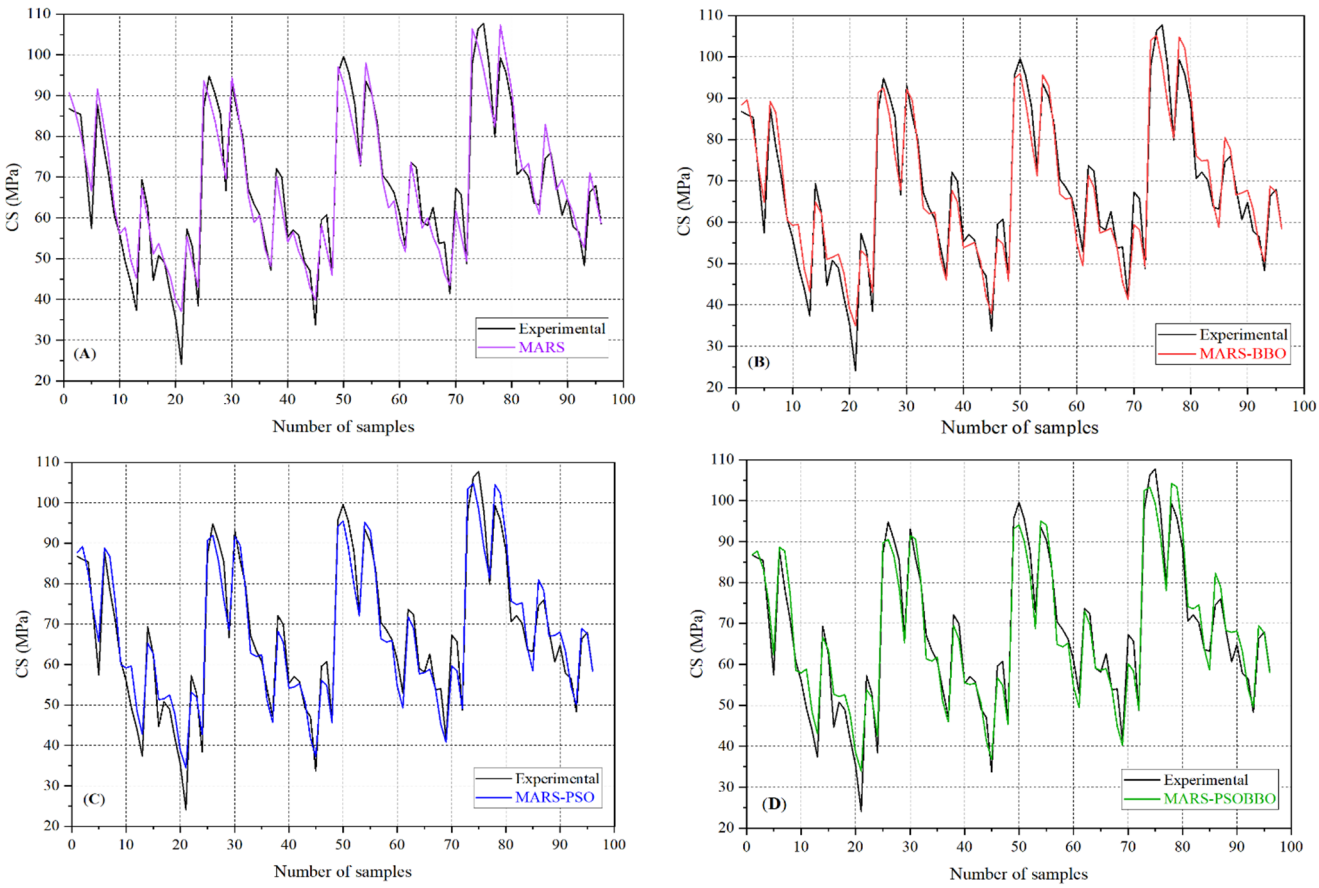

Fig. 9 Experimental and predicted values of CS from (a) MARS; (b) MARS-BBO; (c) MARS-PSO; (d) MARS-PSOBBO

procedure to obtain the most accuracy in predicting CS due to the best performance evaluation results, R^2, RMSE, MAE, and PI equals to 0.9422, 4.3169, 3.5, and 0.0324, respectively.

MARS − PSOBBO:

$$\begin{aligned} f_{CS} = & -665.893 + 1101.84 * \max\left(0, \frac{\mathrm{CA}}{\mathrm{TA}}\right) \\ & + 0.10283 * \max(0, \mathrm{CT} - 28) \\ & + 962.83 * \max\left(0, \frac{\mathrm{CA}}{\mathrm{B}} - 2.851\right) \\ & - 104.183 * \max\left(0, \frac{\mathrm{FA}}{\mathrm{B}} - 0.07325\right) \\ & + 1.052 * \max(0, \mathrm{B} - 414.555) \\ & - 18.7121 * \max\left(0, \frac{\mathrm{SP}}{\mathrm{B}} - 2.0997\right) \end{aligned} \quad (19)$$

References

Adamowski, J.F. (2008), "Development of a short-term river flood forecasting method for snowmelt driven floods based on wavelet and cross wavelet analysis", *J. Hydrol.*, **353**(3-4), 247-266. https://doi.org/10.1016/j.jhydrol.2008.02.013

Atici, U. (2011), "Prediction of the strength of mineral admixture concrete using multivariable regression analysis and an artificial neural network", *Expert Syst. Applicat.*, **38**(8), 9609-9618. https://doi.org/10.1016/j.eswa.2011.01.156

Azimi-Pour, M., Eskandari-Naddaf, H. and Pakzad, A. (2020), "Linear and non-linear SVM prediction for fresh properties and compressive strength of high-volume fly ash self-compacting concrete", *Constr. Build. Mater.*, **230**, p. 117021. https://doi.org/10.1016/j.conbuildmat.2019.117021

Babu, K.G. and Rao, G.S.N. (1994), "Early strength behavior of fly ash concretes", *Cement Concrete Res.*, **24**(2), 277-284. https://doi.org/10.1016/0008-8846(94)90053-1

Behnood, A., Behnood, V., Gharehveran, M.M. and Alyamac, K.E. (2017), "Prediction of the compressive strength of normal and high-performance concretes using M5P model tree algorithm", *Constr. Build. Mater.*, **142**, 199-207. https://doi.org/10.1016/j.conbuildmat.2017.03.061

Benemaran, R.S. and Esmaeili-Falak, M. (2020), "Optimization of cost and mechanical properties of concrete with admixtures using MARS and PSO", *Comput. Concrete, Int. J.*, **26**(4), 309-316. https://doi.org/10.12989/cac.2020.26.4.309

Benhelal, E., Zahedi, G., Shamsaei, E. and Bahadori, A. (2013), "Global strategies and potentials to curb CO_2 emissions in cement industry", *J. Cleaner Prod.*, **51**, 142-161. https://doi.org/10.1016/j.jclepro.2012.10.049

Cabrera, J.G. and Claisse, P.A. (1990), "Measurement of chloride penetration into silica fume concrete", *Cement Concrete Compos.*, **12**(3), 157-161. https://doi.org/10.1016/0958-9465(90)90016-Q

Chou, J.H. and Ghaboussi, J. (2001), "Genetic algorithm in structural damage detection", *Comput. Struct.*, **79**(14), 1335-1353. https://doi.org/10.1016/S0045-7949(01)00027-X

Chou, J.S. and Pham, A.D. (2013), "Enhanced artificial intelligence for ensemble approach to predicting high performance concrete compressive strength", *Constr. Build. Mater.*, **49**, 554-563. https://doi.org/10.1016/j.conbuildmat.2013.08.078

Craven, P. and Wahba, G. (1978), "Smoothing noisy data with spline functions", *Numerische mathematik*, **31**(4), 377-403.

https://doi.org/10.1007/BF01404567
Detwiler, R.J., Bhatty, J.I. and Battacharja, S. (1996), *Supplementary cementing materials for use in blended cements*, No. R&D Bulletin RD112T. http://worldcat.org/isbn/0893121428
Dutta S., Samui, P. and Kim, D. (2018), "Comparison of machine learning techniques to predict compressive strength of concrete", *Comput. Concrete, Int. J.*, **21**(4), 463-470. https://doi.org/10.12989/cac.2018.21.4.463
Esmaeili-Falak, M. (2017), "Effect of system's geometry on the stability of frozen wall in excavation of saturated granular soils", Doctoral Dissertation; University of Tabriz, Tabriz, Iran.
Esmaeili-Falak, M., Katebi, H., Javadi, A. and Rahimi, S. (2017), "Experimental investigation of stress and strain characteristics of frozen sandy soils-A case study of Tabriz subway", *Modares Civil Eng. J.*, **17**(5), 13-23. http://mcej.modares.ac.ir/article-16-7658-en.html
Esmaeili-Falak, M., Katebi, H. and Javadi, A. (2018), "Experimental study of the mechanical behavior of frozen soils-A case study of tabriz subway", *Periodica Polytech. Civil Eng.*, **62**(1), 117-125. https://doi.org/10.3311/PPci.10960
Esmaeili-Falak, M., Katebi, H., Vadiati, M. and Adamowski, J. (2019), "Predicting triaxial compressive strength and Young's modulus of frozen sand using artificial intelligence methods", *J. Cold Regions Eng.*, **33**(3), 04019007. https://doi.org/10.1061/(ASCE)CR.1943-5495.0000188
Esmaeili-Falak, M., Sarkhani Benemaran, R. and Seifi, R. (2020a), "Improvement of the mechanical and durability parameters of construction concrete of the Qotursuyi Spa", *Concrete Res. Quarterly J.*, **13**(2), 81-90. https://doi.org/10.22124/JCR.2020.14518.1395
Esmaeili-Falak, M., Katebi, H. and Javadi, A.A. (2020b), "Effect of freezing on stress–strain characteristics of granular and cohesive soils", *J. Cold Regions Eng.*, **34**(2), 05020001. https://doi.org/10.1061/(ASCE)CR.1943-5495.0000205
Felekoğlu, B., Türkel, S. and Baradan, B. (2007), "Effect of water/cement ratio on the fresh and hardened properties of self-compacting concrete", *Build. Environ.*, **42**(4), 1795-1802. https://doi.org/10.1016/j.buildenv.2006.01.012
Friedman, J.H. (1991), "Multivariate adaptive regression splines", *Annals Statist.*, **19**(1), 1-67. https://www.jstor.org/stable/2241837
Guo, W.A., Li, W.Z., Zhang, Q., Wang, L., Wu, Q.D. and Ren, H.L. (2014), "Biogeography-based particle swarm optimization with fuzzy elitism and its applications to constrained engineering problems", *Eng. Optimiz.*, **46**(11), 1465-1484. https://doi.org/10.1080/0305215X.2013.854349
Hubertova, M. and Hela, R. (2007), "The effect of metakaolin and silica fume on the properties of lightweight self-consolidating concrete", *Special Publication*, **243**, 35-48.
Kennedy, J. and Eberhart, R. (1995), "Particle swarm optimization", *Proceedings of ICNN'95-International Conference on Neural Networks*, Volume 4, pp. 1942-1948. https://doi.org/10.1109/ICNN.1995.488968
Kjellsen, K.O., Wallevik, O.H. and Hallgren, M. (1999), "On the compressive strength development of high-performance concrete and paste—effect of silica fume", *Mater. Struct.*, **32**(1), 63. https://doi.org/10.1007/BF02480414
Khademi, F., Akbari, M., Jamal, S.M. and Nikoo, M. (2017), "Multiple linear regression, artificial neural network, and fuzzy logic prediction of 28 days compressive strength of concrete", *Front. Struct. Civil Eng.*, **11**(1), 90-99. https://doi.org/10.1007/s11709-016-0363-9
Lam, L., Wong, Y.L. and Poon, C.S. (1998), "Effect of fly ash and silica fume on compressive and fracture behaviors of concrete", *Cement Concrete Res.*, **28**(2), 271-283. https://doi.org/10.1016/S0008-8846(97)00269-X
Moayedi, H., Kalantar, B., Foong, L.K., Tien Bui, D. and Motevalli, A. (2019), "Application of three metaheuristic techniques in simulation of concrete slump", *Appl. Sci.*, **9**(20), 4340. https://doi.org/10.3390/app9204340
Mohamed, O.A. and Najm, O.F. (2016), "Splitting tensile strength of self-consolidating concrete containing slag", *Proceedings of AES-ATEMA International Conference, Advances and Trends in Engineering Materials and their Applications*, pp. 109-114. https://doi.org/10.1016/j.proeng.2016.04.157
Mousavi, S.M., Aminian, P., Gandomi, A.H., Alavi, A.H. and Bolandi, H. (2012), "A new predictive model for compressive strength of HPC using gene expression programming", *Adv. Eng Software*, **45**(1), 105-114. https://doi.org/10.1016/j.advengsoft.2011.09.014
Nochaiya, T., Wongkeo, W. and Chaipanich, A. (2010), "Utilization of fly ash with silica fume and properties of Portland cement–fly ash–silica fume concrete", *Fuel*, **89**(3), 768-774. https://doi.org/10.1016/j.fuel.2009.10.003
Oreta, A.W. and Ongpeng, J. (2011), "Modeling the confined compressive strength of hybrid circular concrete columns using neural networks", *Comput. Concrete, Int. J.*, **8**(5), 597-616. https://doi.org/10.12989/cac.2011.8.5.597
Pala, M., Özbay, E., Öztaş, A. and Yuce, M.I. (2007), "Appraisal of long-term effects of fly ash and silica fume on compressive strength of concrete by neural networks", *Constr. Build. Mater.*, **21**(2), 384-394. https://doi.org/10.1016/j.conbuildmat.2005.08.009
Poorjafar, A., Esmaeili-Falak, M. and Katebi, H. (2021), "Pile-soil interaction determined by laterally loaded fixed head pile group", *Geomech. Eng., Int. J.*, **26**(1), 13-25. https://doi.org/10.12989/gae.2021.26.1.013
Sarkhani Benemaran, R. (2017), "Experimental and analytical study of pile-stabilized layered slopes", Thesis; University of Tabriz, Tabriz, Iran.
Sarkhani Benemaran, R., Esmaeili-Falak, M. and Katebi, H. (2020), "Physical and numerical modelling of pile-stabilised saturated layered slopes", *Proceedings of the Institution of Civil Engineers-Geotechnical Engineering*, pp. 1-16. https://doi.org/10.1680/jgeen.20.00152
Shariati, M., Mafipour, M.S., Mehrabi, P., Bahadori, A., Zandi, Y., Salih, M.N., Nguyen, H., Dou, J., Song, X. and Poi-Ngian, S. (2019), "Application of a hybrid artificial neural network-particle swarm optimization (ANN-PSO) model in behavior prediction of channel shear connectors embedded in normal and high-strength concrete", *Appl. Sci.*, **9**(24), 5534. https://doi.org/10.3390/app9245534
Siddique, R. (2004), "Performance characteristics of high-volume Class F fly ash concrete", *Cement Concrete Res.*, **34**(3), 487-493. https://doi.org/10.1016/j.cemconres.2003.09.002
Simon, D. (2008), "Biogeography-based optimization", *IEEE Transact. Evolut. Computat.*, **12**, 702-713. https://doi.org/10.1109/TEVC.2008.919004
Topcu, I.B. and Sarıdemir, M. (2008), "Prediction of compressive strength of concrete containing fly ash using artificial neural networks and fuzzy logic", *Computat. Mater. Sci.*, **41**(3), 305-311. https://doi.org/10.1016/j.commatsci.2007.04.009
Toutanji, H., Delatte, N., Aggoun, S., Duval, R. and Danson, A. (2004), "Effect of supplementary cementitious materials on the compressive strength and durability of short-term cured concrete", *Cement Concrete Res.*, **34**(2), 311-319. https://doi.org/10.1016/j.cemconres.2003.08.017
Turk, K., Turgut, P., Karatas, M. and Benli, A. (2010), "Mechanical properties of selfcompacting concrete with silica fume/fly ash", *Proceedings of the 9th International Congress on Advances in Civil Engineering*, pp. 27-30.
Wang, C.C., Chen, T.T., Wang, H.Y. and Huang, C. (2014), "A predictive model for compressive strength of waste LCD glass

concrete by nonlinear-multivariate regression", *Comput. Concrete*, *Int. J.*, **13**(4), 531-545. http://dx.doi.org/10.12989/cac.2014.13.4.531

Yaprak, H., Karacı, A. and Demir, I. (2013), "Prediction of the effect of varying cure conditions and w/c ratio on the compressive strength of concrete using artificial neural networks", *Neural Comput. Applicat.*, **22**(1), 133-141. https://doi.org/10.1007/s00521-011-0671-x

Yeh, I.C. (1998), "Modeling of strength of high-performance concrete using artificial neural networks", *Cement Concrete Res.*, **28**(12), 1797-1808. https://doi.org/10.1016/S0008-8846(98)00165-3

Zelić, J., Rušić, D. and Krstulović, R. (2004), "A mathematical model for prediction of compressive strength in cement–silica fume blends", *Cement Concrete Res.*, **34**(12), 2319-2328. https://doi.org/10.1016/j.cemconres.2004.04.015

CC

Notation

CS	Compressive strength
HPC	High-Performance Concrete
B	binder content
FA/B	fly ash to binder ratio
SF/B	Silica fume to binder ratio
CA/B	coarse aggregate to binder ratio
CA/TA	coarse aggregate to total aggregate ratio
W/B	water to binder ratio
SP/B	superplasticizer to binder ratio
CT	Curing time
MARS	Multivariate adaptive regression splines
BBO	Biogeography-based optimization
PSO	Particle swarm optimization